

# Analysis of Magneto-Thermal-Solid Coupling Field in a Deflectable Double-Stator SRG

Zheng Li<sup>1</sup>, Lei Du<sup>1</sup>, Xin Wang<sup>1</sup>, Liping Zhang<sup>1</sup>, Qunjing Wang<sup>2</sup>

<sup>1</sup>School of Electrical Engineering, Hebei University of Science and Technology, Shijiazhuang, China; <sup>2</sup>National Engineering Laboratory of Energy-saving Motor & Control Technique, Anhui University, Hefei, China

## Abstract

In order to improve the utilization of wind energy, a new type of deflectable double-stator switched reluctance wind power generator is proposed for the single of the rotor rotation of the existing Switched Reluctance Generator. The generator adopts inner and outer double-stator structure, the rotor shaft and the inner stator connecting shaft are connected with the relevant section bearing, which can realize the rotor deflection in a certain range, adapt to different wind directions and is suitable for various wind power generation occasions, and can improve the working efficiency of the generator. Through the simulation calculation of the coupling of the electromagnetic field, temperature field and stress field, and the comparison of unidirectional and bidirectional coupling of electromagnetic field and temperature field, the temperature rise of the designed structure, the stress due to thermal expansion and the corresponding vibration displacement are obtained. In addition, through the comparative analysis of experimental measurements and simulation data, the temperature difference is little, which verifies the correctness of the simulation. It provides a reference for studying the multi-physical field coupling calculation of generators, optimizing the structure of such generators and improving the stability of their operation.

**Keywords:** Multiple physical field coupling; Bidirectional coupling; Vibration displacement; Double-stator; Deflection

*Received:* 19 February 2019

## To cite this article:

Zheng Li, Lei Du, Xin Wang, Liping Zhang, Qunjing WANG, "Analysis of Magneto-thermal-solid Coupling Field in a Deflectable Double-stator SRG", in *Electrotehnica, Electronica, Automatica (EEA)*, 2020, vol. 68, no. 1, pp. 68-75, ISSN 1582-5175.

## 1. Introduction

Switched Reluctance Wind Turbine has the advantages of simple and compact structure, low starting wind speed and stable output power. Therefore, it has broad application prospects and high research value in the field of wind power generation. The generator with double-stator structure has fast response, high precision positioning and strong overload ability, and its working efficiency can be greatly improved when the generator body structure and external wind speed are fixed.

Literature [1] gives a brief introduction to the structure types of double-stator motors, research status and the development trends at home and abroad.

Literature [2] presents a new type of double-stator low-speed rare earth permanent magnet synchronous generator. It is concluded that the output characteristics of the double-stator structure generator are better than that of the single-stator structure.

Literature [3] presents a three-degree-of-freedom motor driven by permanent magnet, which improves the torque characteristics of the motor.

At the same time, according to the previous deflectable multi-degree-of-freedom motor [4-6], it has the advantages of high efficiency and high flexibility.

Based on the research contents of the above literature, a deflectable double-stator SRG is proposed in this paper. In addition to the rotor and double-stator design with cogging structure on both sides of the rotor, the special structure of one side of the rotor is used to adjust the steering of the generator to adapt to different wind directions and improve the utilization of wind energy. Its main feature is the use of a rotor with a cogging structure on both sides and the design of double-stator, the special structure on one side of the rotor is used to adjust the direction of the generator in order to adapt to different wind directions and improve the utilization rate of wind energy.

With the development of motor manufacturing level, the theory and research of motor temperature rise have been progressing.

Before the 1970s, simplified formulas were the main method for calculating the heat of motors. The calculation accuracy is poor and only the average temperature rise of the motor can be calculated, which cannot meet the needs of the design work.

At the same time, the thermal model of motor was established by equivalent thermal circuit method in the early stage, which can be traced back to 1920.

In 1955, a small number of scholars used equivalent thermal circuit method to study the temperature rise of

motor. This method is more accurate than the simplified formula method and can obtain the overall temperature rise distribution and average temperature rise of the motor.

Referring to the traditional thermal circuit diagram model of the SRM, a three-dimensional equivalent thermal network model is established in reference [7-8], which provides a basis for the temperature rise calculation of the SRM, but if want to improve the accuracy of calculation, it is needed to increase the number of network nodes and thermal resistance, which will greatly increase the workload, and will lose the characteristics of small calculation workload.

In recent years, the application of finite element method in thermal analysis has become more and more mature. It transfers the research object from the whole to the local element, and solves the heat conduction equation [9-11] by using modern numerical method, so that every local element in the whole calculation area can obtain reliable calculation data, which can guide the design of motor more accurately and reasonably.

In this paper, the FEM is used to study the thermal, electrical and structural multiple physical field vibration of the SRG.

The COMSOL finite element platform is used to simulate and analyse the temperature rise of the generator, the stress of the double-stator under thermal expansion and the vibration displacement caused by thermal expansion. variable

The result provides a theoretical reference for further optimization of the generator.

## 2. Materials and Methods

### 2.1 Overall structure and modelling parameters of the generator

The deflectable double-stator switched reluctance generator body structure was composed of inner and outer double-stator, a rotor, and a concentrated winding wound on the inner and outer double-stator teeth poles.

The inner side of the outer stator core was concave spherical, while the outer side of the inner stator core was convex spherical.

The rotor was located between the inner and outer stators, with concave spherical and convex spherical outlines respectively, and the inner and outer surfaces of the rotor core were equipped with eight rotor teeth poles.

That was, a three-phase generator with 12 / 8 / 8 / 12 poles.

The internal structure is shown in Figure 1.

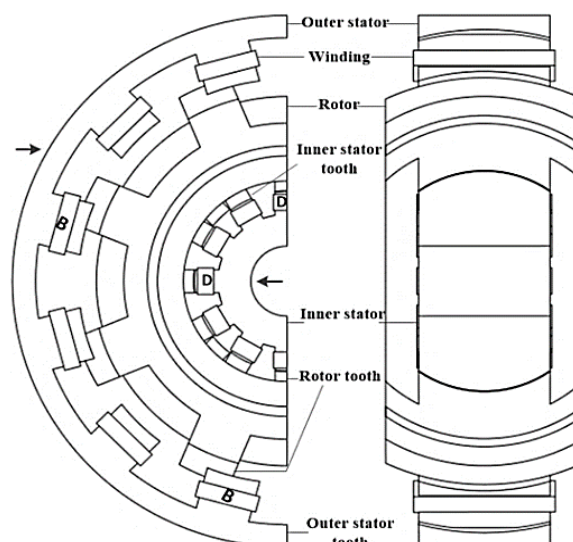


Figure 1. Internal structure of the generator

The main structural parameters of the deflectable double-stator SRG were shown in Table 1.

Table 1. Main structural parameters of a double-stator SRG

$D_{s1}=167\text{mm}$	Outer diameter of the outer stator
$D_{s2}=37\text{mm}$	Inner diameter of inner stator
$D_{r1}=116\text{mm}$	Outer diameter of Rotor
$D_{r2}=87\text{mm}$	Inner diameter of Rotor
$G=0.5\text{ mm}$	Inner and Outer air gaps
$H_{cs1}=9$	Height of Outer stator yoke
$H_{cs2}=20$	Height of Inner stator yoke
$N_s=12$	Number of Stator teeth
$N_r=8$	Number of Rotor teeth
$H_{cr}=100\text{mm}$	Height of Rotor yoke
$L_a=90\text{mm}$	Iron core length

The arrow showed the position indicated by the fixed constraint. The outer diameter surface of the outer stator was fixed on both sides of the outer shell of the generator, and the inner diameter surface of the inner stator was fixed on the base of the generator housing through the connecting shaft base of the inner stator.

### 2.2 Working principle of the generator

According to the structure of generator, it can be approximately regarded as consisting of internal and external generators. That was an outer stator and an inner rotor forming an inner rotor SRG, the inner stator and the outer rotor composing an outer rotor SRG.

As the structure of the generator was an internal and external double-stator, two sets of external control circuits were used to connect the inner stator windings (D, E, F) and the outer stator windings (A, B, C).

The generator rotor was driven by the prime mover to rotate and control the motor to realize the conversion of excitation and generator freewheeling.

The counter-clockwise direction was defined as the positive direction of motor rotation. When the rotor

position was in the range of  $(17.5^\circ - 27.5^\circ)$ , the inner stator D-phase winding was turned on when the rotor position is was the  $(25^\circ - 35^\circ)$  interval, the outer stator B phase winding was connected. In this paper, the rotor position angle WS  $38^\circ$ .

At that time, the rotor was in the middle position relative to the outer stator, that was, the rotor tooth pole and the outer stator tooth pole partially overlap.

The D-phase winding of the inner stator and the outer-phase stator B-phase winding were simultaneously.

In the power generation state, the generation current of the B-phase winding was 25 A, and the power generation current of the D-phase winding was 13 A.

Figure 1 (*supra*) showed the structure diagram of the generator when the rotor rotated 38 degrees anticlockwise. Because it was a 12/8/8/12 pole three-phase generator, and there were four generator windings D and B on the inner and outer double-stator, which were  $\pi / 2$  apart from each other.

### 2.3 Theoretical analysis of magnetic field, heat source and heat transfer of the generator

After generator B and D phase windings generated electricity, electromagnetic field was established in the air gap between stator and rotor salient pole.

The loss obtained by magnetic field analysis was the heat source of thermal analysis. The loss obtained by magnetic field analysis was the heat source of thermal analysis.

According to the mechanism of heat transfer, there were three basic ways of heat transfer. Heat conduction, convection and radiation. When SRG was analysed, the copper and iron losses inside the motor were accurately obtained, and then coupled to the temperature field of the generator as an internal heat source. Only heat conduction and heat convection were considered to transfer heat to the generator body. Based on the theory of heat transfer, the distribution of temperature field inside the generator was obtained by magnetic-thermal-coupled simulation.

#### 2.3.1 Magnetic field analysis

When the four windings of the B phase of the generator generated electricity, the power supply exerted excitation voltage to the windings, and the phase current gradually increased and formed a magnetic field.

The magnetic field equation of the motor winding was as follows:

$$\begin{cases} \nabla \cdot H = J \\ \nabla \cdot E = -\frac{\partial B}{\partial t} \\ \sigma \frac{\partial A}{\partial t} + \nabla \cdot (\sigma \cdot \nabla \cdot A) = J \\ B = \nabla \times A \end{cases} \quad (1)$$

where:

- $J$  was the source current density;
- $B$  was magnetic induction intensity;
- $E$  was the intensity of electric field;
- $H$  was the intensity of magnetic field;

- $A$  was vector magnetic potential;
- $\sigma$  was the conductivity.

### 2.4 Heat source analysis

Heat transfer loss analysis was not only the basis of temperature field analysis in the motor, but also the key to improve the efficiency of the generator.

It can be concluded that accurate calculation of motor losses was of great significance for improving motor performance, protecting motor and optimizing design.

Motor losses can be divided into stator core losses, additional losses, mechanical losses, copper losses and stray losses caused by current in windings. Because the calculation of mechanical loss and additional loss was more complex, and the proportion of total loss is small, this paper mainly studied iron loss and copper loss. Among them, iron loss included hysteresis loss, eddy current loss and additional loss.

The calculation formula was as follows [12-15].

$$P_{Fe} = P_h + P_e + P_r = C_h f B_m^2 + C_e f^2 B_m^n \quad (2)$$

where:

- $P_{Fe}$  was the total core loss;
- $C_h$  was the hysteresis loss coefficient;
- $C_e$  was the eddy current loss coefficient;
- $f$  was the frequency of sinusoidal flux;
- $B_m$  was the average flux density amplitude.

When  $B_m < 1$ ,  $n$  take 1.6, when  $B_m > 1$ ,  $n$  take 2; the value of  $P_r$  was neglected.

When the generator ran in steady state, the skin effect on the coil surface was neglected, and the total copper consumption of the winding was as follows:

$$P_{Cu} = m I_{rms}^2 R \quad (3)$$

where:

- $m$  was the number of motor phases;
- $I_{rms}$  was the effective value of winding phase current;
- $R$  was the value of phase winding resistance.

SRG would produce a large number of copper and iron losses during operation, which would lead to the rise of temperature of stator, rotor and winding.

Excessive temperature would not only reduce the efficiency of the motor, but also accelerate the aging of winding insulation and reduce the service life.

Therefore, accurate calculation of inner losses of SRG had important practical value for improving generator performance and reliable operation.

### 2.5 Theoretical analysis of the heat transfer

“Joule heat and thermal expansion” multi-physical field interface combined electromagnetic field, temperature field and stress field, and coupled copper and iron losses from electromagnetic analysis of the previous section to temperature field as heat source [16-18]. From the coupled analysis of electromagnetic-temperature field, it can be seen that the equation of electromagnetic heat source was as follows:

$$\begin{cases} \rho C_p u \cdot \nabla T = \nabla \cdot (k \nabla T) + Q_e \\ Q_e = J \cdot E \end{cases} \quad (4)$$

Firstly, the  $B$  and  $D$  power generation coils conducted heat to the surface of the element through heat conduction, and then scattered it to the surrounding medium through convection and radiation.

Thermal conduction and convection played an important role in the process of heat transfer in the generator. The heat conduction equation was:

$$\begin{cases} \rho C_p u \cdot \nabla T + \nabla \cdot q = Q \\ q = -k \nabla T \end{cases} \quad (5)$$

where:

- $Q$  was the heat source;
- $\rho$  was the density;
- $C_p$  was the heat capacity;
- $K$  was the heat conduction coefficient.

There was a heat transfer relationship between the heat conduction system of the generator body and the surrounding medium, that was called boundary conditions, to distinguish the surrounding medium from the generator body.

The generator stator system was transferred to the rotor by thermal convection.

The convective air cooling in other boundary was simulated by using heat flux boundary conditions with heat transfer coefficient  $h$  of  $5W/(m^2K)$  and external temperature  $T_{ext}$  of  $293.15 [K]$ . The heat flux boundary conditions were as follows:

$$\begin{cases} -n \cdot q = q_0 \\ q_0 = h(T_{ext} - T) \end{cases} \quad (6)$$

Expansion Deformation of Generator Body Caused by Rising Temperature, as a coupling interface, the governing equation of thermal expansion was as follows:

$$\varepsilon_{th} = \alpha(T)(T - T_{ref}) \quad (7)$$

where:

$T_{ref}$  set the strain reference temperature equal to the external temperature  $T_{ext}$ .

Thermal expansion caused stress in the generator body. Thermal expansion was a volume force load in structural mechanics analysis, under which the driving motor would experience stress.

The governing equation of stress was as follows:

$$F = E\alpha(T - T_{ref}) \quad (8)$$

## 2.6 The mode of coupling

There are two coupling modes between magnetic field and temperature field, one was unidirectional coupling and the other was bidirectional coupling. The research method of this paper was bidirectional coupling.

The concept of the unidirectional coupling was that all the final analysis results of one physical field were directly coupled to another. For example, in the

electromagnetic field and temperature field, the loss of the generator generated electromagnetic field was coupled to the temperature field as the heat source of the temperature field analysis, and whether the result of the temperature field solution had any impact on the electromagnetic field was not considered.

The concept of the Bidirectional coupling was that data exchange between two physical fields.

For example, the loss obtained from the magnetic field analysis was coupled to the temperature field as the heat source required by the thermal analysis in Section 2.4.

The result obtained from the temperature field analysis affected the resistivity of the magnetic material in the magnetic field analysis, and it would cycle until the generator reaches the thermal balance, and finally the corresponding result would be obtained[19, 20].

The coil in this paper was wound by copper wire, assuming that the conductivity was constant, and the resistance of conductor increases with the increase of temperature.

The relationship between resistivity and temperature was approximately linear over a large range.

$$\rho = \rho_0(1 + \alpha(T - T_{ref})) \quad (9)$$

$$\sigma = 1/\rho \quad (10)$$

where:

- $\alpha$  was the temperature coefficient;
- $\rho_0$  was the reference resistivity of copper and set at  $1.75 \times 10^{-8}(\Omega \cdot m)$ ;
- $\sigma$  was the conductivity.

According to the relation of resistivity defined in formula (9), the temperature dependence of conductor can be obtained, and the conductivity was the reciprocal of resistivity.

## 3. Results

### 3.1 Coupling analysis of the electromagnetic field-temperature field and the stress field of the stator structure

In this paper, the coupled numerical modes of electromagnetic field-temperature field-stress field was established. In order to obtain the temperature rise under the loss as heat source, the stress of stator system under thermal expansion and the vibration displacement under thermal stress in the finite element analysis, the theory of electromagnetic field, loss and heat transfer was analysed in the last section.

#### 3.1.1 Analysis of the results of the external stator

Since the generator was a deflectable double-stator structure, this section first analysed the influence of the generator coil on the multi-physical field coupling of the external stator.

In the finite element simulation, the contact part between the outer stator and the surface of the outer stator shell was set as a boundary condition, which was called fixed constraints. It is shown by the arrow on the left side of Figure 1 (*supra*).

When the B-phase winding on the external stator generated electricity, the bidirectional coupling analysis was carried out first.

Let the temperature coefficient  $\alpha = 0.0039 \text{ 1/k}$  be substituted into equation (9), and the correlation between resistivity and temperature  $T$  was shown in equation (9). It was the temperature distribution obtained by Bidirectional coupling analysis.

The results obtained were shown in the graphs below.

The temperature changes caused by copper and iron losses of the generator external stator were shown in Figure 2.

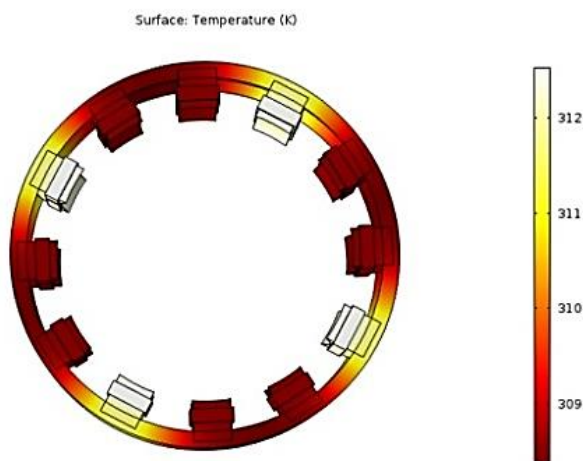


Figure 2. Bidirectional coupled temperature distribution map

The stress caused by thermal expansion of the structure are shown in Figure 3.

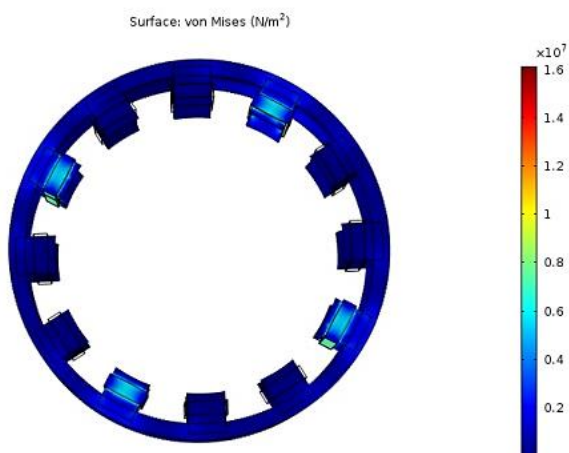


Figure 3. Stress distribution diagram of outer stator

Then the constant resistivity and temperature coefficient  $\alpha = 0 \text{ 1/k}$  were substituted into equation (9) for comparison with the strong coupling data.

The temperature of the generator stator was obtained as shown in Figure 4.

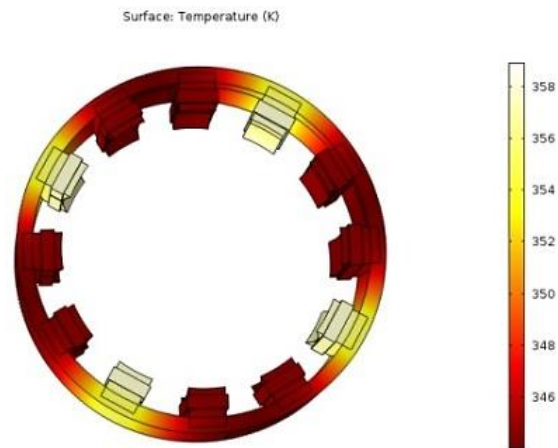


Figure 4. Unidirectional Coupled Temperature Distribution Map

### 3.1.2 Analysis of the results of the inner stator

The influence of generator coil on multi-physical field coupling of external stator was analysed in the last section.

Similarly, the part where the inner stator contacts the inner stator axis was set as a boundary condition. It was shown by the arrow on the right side of Figure 1 (*supra*).

In addition, there were 12 inner stator teeth on the inner stator of the generator.

According to the analysis of Figure 2 (*supra*), the influence of four B-phase coils on the external stator structure only concentrated on the external stator teeth and the external stator yoke, which had no effect on the adjacent stator teeth.

Therefore, this section only analysed the power generation of four D-phase power generating windings on the inner stator teeth. The remaining 8 inner stator teeth and windings were not studied because they did not generate electricity.

The temperature variation caused by copper and iron losses were shown in Figure 5.

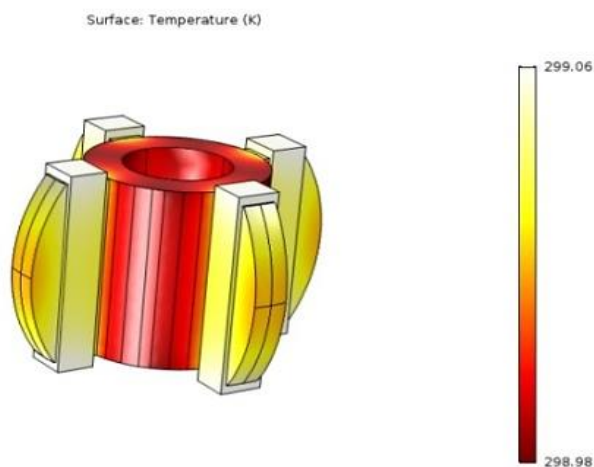


Figure 5. Bidirectional Coupled Temperature Diagram

We noted that the maximum temperature of the internal stator of the generator was 299.06 K, and due

to the effect of heat conduction and convection, the temperature at different positions of the internal stator was different.

The stress caused by thermal expansion of the structure in the generator was shown in Figure 6.

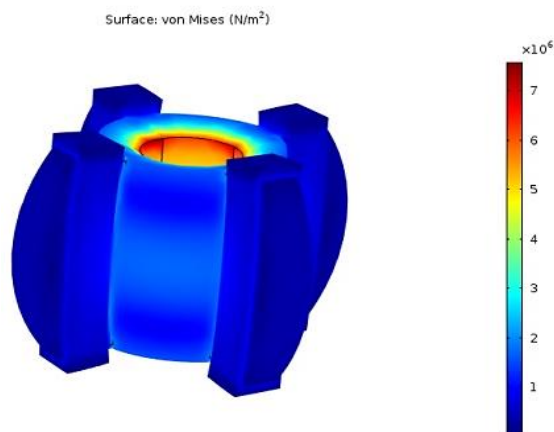


Figure 6. Stress distribution diagram of inner stator

It can be seen from the observation of the Figure 6, that from the fixed constraint to the inner stator, the stress on the inner stator gradually decreased, and the stress on the stator teeth was the smallest.

The red line and blue line in Figure 7 were the vibration displacement curves of the outer diameter of the inner stator with unidirectional coupling and bidirectional coupling respectively.

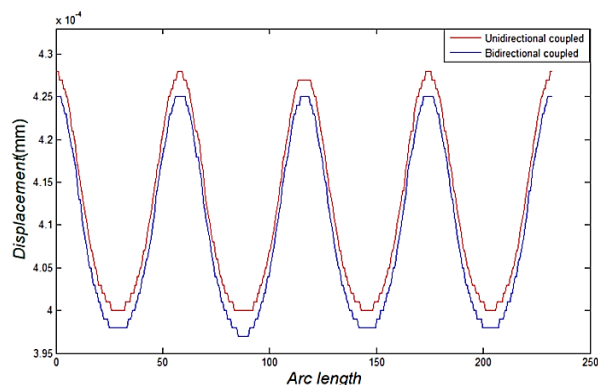


Figure 7. Displacement Contrast Diagram

In Figure 7, the vibration displacement of the red line was larger than that of the blue line.

#### 4. Discussion

The study of this paper was a deflectable double stator Switched Reluctance Wind turbine.

Due to the limited space, only the temperature analysis and stress situation related to the outer stator and the inner stator were analysed, while the stator structure did not analyse the temperature rise and vibration of the rotor, and also did not do too much analysis on the generator in the case of deflection, which would be analysed in the future research.

#### 4.1 External stator analysis

Analysis of Figure 2 (*supra*) showed that the stator tooth temperature of the four B phase windings of the external stator was the highest, which was about 313K. Temperature transferred heat from the heat source to the rest of the stator structure through heat conduction.

Under the combined action of copper loss and stator iron loss, this leading to the different parts of the generator had different temperatures.

From the observation of Figure 3 (*supra*), it can be seen that the external stator of the generator was subjected to the greatest stress around the four B-phase generating windings, which was about  $1.6 \times 10^7$  N/m<sup>2</sup>, corresponding to the temperature distribution of the external stator.

It can be seen from Figure 4 (*supra*), that the maximum temperature of the external stator was 359 K when unidirectional coupling analysis was carried out.

Compared with the Bidirectional coupling temperature of Figure 2 (*supra*), the maximum temperature increased by almost 46 K at this time.

#### 4.2 Inner stator analysis

It can be seen from the Figures 5 and 6 (*supra*), that the stress was high in the place where the temperature is high. Since the fixed constraint was the position indicated by the arrow on the right side of Figure 1 (*supra*), the maximum stress on the inner stator was concentrated at the fixed constraint, which was about  $7.2 \times 10^4$  N/m<sup>2</sup>.

#### 4.3 Comparative analysis of single and two-way coupled vibration

It can be seen from the Figure 7 (*supra*), that the unidirectional coupling was higher than the bidirectional coupling temperature rise in the previous section.

According to the vibration displacement generated by thermal expansion, the vibration displacement of the temperature rise was larger, which was consistent with the actual situation.

#### 5. Conclusion

Based on the electromagnetic field-temperature field-stress field module, through the theoretical analysis of magnetic field, heat source and heat transfer, FEA was used to intuitively model the generator.

In this paper, the two-way coupling of magnetic field and temperature field was used to analyse the temperature rise of the generator.

The inner diameter vibration displacement of the inner stator of the generator was compared with that of the single-way coupling and the two-way coupling.

It can be seen that the vibration displacement increased with the increase of temperature.

This paper systematically expounds the heat source as loss, the stress on the stator system caused by thermal expansion and the corresponding vibration displacement, which are small and have no effect on the normal operation of the generator.

The stator yoke and teeth in the stator structure suffer more stress than other parts of the stator structure.

In order to ensure the long life of the generator, the influence of temperature dependent resistivity on the solution cannot be ignored.

In addition, the above analysis shows that the two-way coupling is much closer to the fact than the one-way coupling and can predict the temperature distribution in the generator more accurately.

The thermal stress will produce load on the material and will cause vibration displacement of the stator system.

Therefore, the strength of the structural material should be increased in the corresponding parts of the stator system to prevent damage to the motor structure due to excessive stress, which can improve the operation stability of the generator and reduce vibration and noise.

In addition, the vibration displacement is very small and has little effect on the work of the generator.

From the perspective of electromagnetic field-temperature field-stress field, it can predict the fault diagnosis and state detection of generator.

The research content of this paper provides a theoretical basis for the optimal design of motor in the future.

## 6. Bibliographic References

- [1] FENG, C., SHU MEI, C., SHU KANG, C., "Development and Expectation of Double Stator Electric Machine", in *Small & Special Machines*, 2001.
- [2] XIPING, L., XIAO HAI, H., "Design of a Novel Double-stator Permanent Magnet Synchronous Wind Generator with Low Speed", in *Micromotors Servo Technique*, 2006.
- [3] ZHENG L., QING QING L., DIAN HUI X., "Design and implementation of a three-degrees-of-freedom deflection type PM motor", in: Magnetics Conference, Beijing, China, 11-15 May. 2015, IEEE, 2015.
- [4] ZHENG, L., YONG TAO, W., RONG LIANG, G., "The Summary and Latest Research of PM Spherical M-DOF Motor", in *Micromotors*, 2011.
- [5] LU, K., "Statistical moment analysis of multi-degree of freedom dynamic system based on polynomial dimensional decomposition method", in *Nonlinear Dynamics*, 2018, vol. 93, no. 4, pp. 2003-2018, ISSN 0924-090X.
- [6] YANG LING, LI., HAO, D., YANG, M., "Two-Degree-Of-Freedom H $\infty$  Robust Control Optimization for IPT System with Parameter Perturbations", in *IEEE Transactions on Power Electronics*, 2018, vol. 33, no. 12, pp. 10954-10969, ISSN 0885-8993.
- [7] YI QIANG, FU., HUA JIANG, O., DAVIS, R. B., "Nonlinear dynamics and triboelectric energy harvesting from a three-degree-of-freedom vibro-impact oscillator", in *Nonlinear Dynamics*, 2018, vol. 92, no. 4, pp. 1985-2004, ISSN 0924-090X.
- [8] HONG FENG, L., YAN BO, S., "Thermal Analysis of the Permanent-Magnet Spherical Motor", in *IEEE Transactions on Energy Conversion*, 2015, vol. 30, no. 3, pp. 1-8, ISSN 0885-8969.
- [9] NAN NAN, Z., WEI GUO, L., "Electromagnetic Field and Thermal Field Coupling Analysis of Brushless DC Motor", in *Small and Special Electrical Machines*, 2009, vol. 37, no. 3, pp. 9-11.
- [10] YIN, L., YA DONG, G., YAO, S., "Simulation of Temperature Field for Bulk Metallic Glass in Micro-scale Grinding", in *Journal of Northeastern University*, 2018, vol. 39, no. 6, pp. 014, ISSN 1005-3026.
- [11] WANG, X., JIA, Z., GAO P., "Coupled electromagnetic-thermal field analysis of out-rotor in-wheel motor", in *Journal of Tianjin University*, 2014, vol. 47, no. 10, pp. 898-902.
- [12] TAO, H., JIANG JUN R., YU JIAO, Z., "Multi-phase Asynchronous Motor Design Platform based on Coupled Field Analysis", in *Large Electric Machine & Hydraulic Turbine*, 2012.
- [13] HONG FENG, L., SHEN, Y., "Thermal Analysis of the Permanent-Magnet Spherical Motor", in *IEEE Transactions on Energy Conversion*, 2015, vol. 30, no. 3, pp. 1-8, ISSN 0885-8969.
- [14] XU ZHEN, H., QIANG, T., LI YI, L., "Winding Temperature Field Model Considering Void Ratio and Temperature Rise of a Permanent-Magnet Synchronous Motor With High Current Density", in *IEEE Transactions on Industrial Electronics*, 2017, vol. 64, no. 3, pp. 2168-2177, ISSN 0278-0046.
- [15] ZHENG, Z., HAO, Y., DONG BO, C., "Machine-Thermal Coupling Stresses Analysis of the Fin-Type Structural Thermoelectric Generator", in *Journal of Electronic Materials*, 2017, vol. 46, no. 5, pp. 3156-3165, ISSN 0361-5235.
- [16] LI PING, H., ZHU, H., BAO KUANG, L., "Temperature Distribution and Thermal Deformation of the Crystallization Roller Based on the Direct Thermal-Structural Coupling Method", in *JOM*, 2017, vol. 69, no. 3, pp. 1-7, ISSN 1047-4838.
- [17] OKA, T., HIROSE, Y., KANAYAMA, H., "Performances of compact magnetic field generators using cryo-cooled high temperature bulk superconductors as quasi-permanent magnets", in *Superconductor Science & Technology*, 2007, vol. 20, no. 12, pp. 1233-1238, ISSN 0953-2048.
- [18] WEI, L., TIAN, J., "Unsteady-state temperature field and sensitivity analysis of gear transmission", in *Tribology International*, 2017, vol. 116, no. 7, pp. 229-243, ISSN 0301-679X.
- [19] Kim, Yong Jae., "Anthropomorphic Low-Inertia High-Stiffness Manipulator for High-Speed Safe Interaction", in: *IEEE Transactions on Robotics*, 2017, vol. 33, no. 6, pp. 1358-1374, ISSN 1552-3098.
- [20] Lu, Z., Huang, P., and Liu, Z. "Predictive Approach for Sensorless Bimanual Teleoperation under Random Time Delays with Adaptive Fuzzy Control", in: *IEEE Transactions on Industrial Electronics*, 2018, vol. 65, no. 3, pp. 2439-2448, ISSN 0278-0046.

## 7. Funding Sources

This work was financially supported by the National Natural Science Foundation of China (51877070, 51577048); Hebei Provincial Natural Science Foundation Project (E2018208155); the Talent Engineering Training Support Project of Hebei Province (A201905008); Hebei Province Higher Education Science and Technology Research Key Project (ZD2018228); High-energy-saving Motor and Control Technology National and Local Joint Engineering Laboratory Open Project (KFKT201901), Hebei Province Graduate Innovation Funding Project (CXZZSS2018085, CXZZSS2019084).

## 8. Authors' Biography



**Zheng Li** was born in Shijiazhuang (China), on 1980.

He received the Ph.D. degree in power electronics and electrical drive from Hefei University of Technology (China), in 2007.

Currently, He is a Professor at Hebei University of Science and Technology, in Shijiazhuang (China).

His major research interests concern: design, analysis, and control of novel motors and actuators, intelligent control, and power electronics.

*e-mail address:* Lizheng@hebust.edu.cn; Lzhfgd@163.com



**Lei Du** was born in Zhangjiakou (China), on 1992.

He received the B.Sc. degree in electrical engineering and automation from Hebei University of Science and Technology (China), in 2017.

Currently, He is a graduate student at Hebei University of Science and Technology, in Shijiazhuang (China).

His major research interests: modelling and control of manipulator, renewable energy applications.

*e-mail address:* dulei@stu.hebust.edu.cn



**Xin Wang** was born in Cangzhou (China), on 1991.

She received the B.Sc. degree in electrical engineering and automation from Hebei University of Science and Technology (China), in 2017.

Currently, She is a graduate student at Hebei University of Science and Technology, in Shijiazhuang (China).

She major research interests concern: switched reluctance generator and its control method.

*e-mail address:* wangxin@stu.hebust.edu.cn



**Liping Zhang** was born in Langfang (China), on 1992.

She received the B.Sc. degree in electrical engineering and automation from Hebei University of Science and Technology (China), in 2017.

Currently, She is a graduate student at Hebei University of Science and Technology, in Shijiazhuang (China).

Her major research interests concern: battery SOC estimation, modeling and renewable energy applications in the DC microgrid.

*e-mail address:* zhangliping@stu.hebust.edu.cn



**Qunjing Wang** was born in Bengbu (China), on 1960.

He received his Ph.D. degree in Electrical Engineering from University of Science and Technology of China (China), 2000.

Currently, He is a Professor and Doctoral Supervisor at National Engineering Laboratory of Energy-saving Motor & Control Technique, Anhui University, in Hefei (China).

His major research interests include the special PM motor and its drive system.

*e-mail address:* wangqunjing@ahu.edu.cn